

# 1 **Assessment of biomass energy potential for SRC willow woodchips** 2 **in a pilot scale bubbling fluidized bed gasifier**

3  
4 Irfan Ul Hai<sup>a</sup>, Farooq Sher<sup>b,\*</sup>, Aqsa Yaqoob<sup>a,c</sup>, Hao Liu<sup>a</sup>

5 *a. Faculty of Engineering, University of Nottingham, Nottingham NG7 2RD, UK*

6 *b. School of Mechanical, Aerospace and Automotive Engineering, Faculty of Engineering,*  
7 *Environmental and Computing, Coventry University, Coventry CV1 2JH, UK*

8 *c. Department of Chemistry, University of Agriculture, Faisalabad 38000, Pakistan*  
9

## 10 **Abstract**

11 The current study investigates the short rotation coppice (SRC) gasification in a bubbling fluidized bed  
12 gasifier (BFBG) with air as gasifying medium. The thermochemical processes during combustion were  
13 studied to get better control over the air gasification and to improve its effectiveness. The combustion  
14 process of SRC was studied by different thermo-analytical techniques. The thermogravimetric analysis  
15 (TGA), derivative thermogravimetry (DTG), and differential scanning calorimetry (DSC) were  
16 performed to examine the thermal degradation and heat flow rates. The product gas composition (CO,  
17 CO<sub>2</sub>, CH<sub>4</sub> and H<sub>2</sub>) produced during gasification was analyzed systematically by using an online gas  
18 analyzer and an offline GC analyzer. The influence of different equivalence ratios on product gas  
19 composition and temperature profile was investigated during SRC gasification. TG/DTG results  
20 showed degradation occur in four stages; drying, devolatilization, char combustion and ash formation.  
21 Maximum mass loss ~70% was observed in devolatilization stage and two sharp peaks at 315–500 °C  
22 in TG/DSC curves indicate the exothermic reactions. The temperature of gasifier was increased in the  
23 range of 650–850 °C along with the height of the reactor with increasing equivalent ratio (ER) from  
24 0.25 to 0.32. The experimental results showed that with an increment in ER from 0.25 to 0.32, the

---

\* Corresponding author: Tel.: +44 (0) 24 7765 7754

E-mail address: [Farooq.Sher@coventry.ac.uk](mailto:Farooq.Sher@coventry.ac.uk) (F.Sher)

25 average gas composition of H<sub>2</sub>, CO, CH<sub>4</sub> decreased in the range of 9–6%, 16–12%, 4–3% and CO<sub>2</sub>  
26 concentration increased from 17–19% respectively. The gasifier performance parameters showed a  
27 maximum high heating value (HHV) of 4.70 MJ/m<sup>3</sup>, Low heating value (LHV) of 4.37 MJ/m<sup>3</sup> and cold  
28 gas efficiency (CGE) of 49.63% at 0.25 ER. The ER displayed direct effect on carbon conversion  
29 efficiency (CCE) of 95.76% at 0.32 ER and tar yield reduced from 16.78 to 7.24 g/m<sup>3</sup> with increasing  
30 ER from 0.25 to 0.32. All parametric results confirmed the reliability of the gasification process and  
31 showed a positive impact of ER on CCE and tar yield.

32

33 **Keywords:** Renewable energy; Biomass gasification; Bubbling fluidized bed; SRC willow chips;  
34 Thermo-analytical techniques; Product gas composition and tar yield.

35

## 36 **1 Introduction**

37 The growing energy demand from coal and natural gas leads to a shortage of fossil fuel because  
38 of time constraint for its reproducibility and environmental issues regarding fossil's fuel emission:  
39 the greenhouse effect and global warming in the near future. Biomass is a preferable energy source  
40 due to abundantly available, easily storable, transportable, and independent of location and climate  
41 [1]. Biomass is considered as the fourth renewable, potentially sustainable source of alternative  
42 energy which meets 14% of the total world's primary energy consumption [2]. It was reported that  
43 4.8 G tons of oil equivalent biomass will be used as a source of fuel in 2050 [3]. Biomass is a  
44 carbon-neutral energy source with zero CO<sub>2</sub> emissions [4, 5]. During the combustion of biomass  
45 fuels, useful energy and the same amount of CO<sub>2</sub> is released which was absorbed during the plant  
46 life cycle and emissions of SO<sub>2</sub> and NO<sub>x</sub> are extremely low. Therefore, biomass is a good choice  
47 as a clean and environment friendly fuel after coal and natural gas [6].

48

49 The selection of biomass fuel is dependent on ash/ residue contents, moisture contents,  
50 cellulose/lignin ratio, carbon and volatiles, alkali metal contents, calorific value and moisture  
51 contents [7, 8]. The process of ignition becomes difficult when the biomass moisture contents are  
52 more than 30% [9]. Thermochemical conversion (combustion, pyrolysis and gasification) while  
53 biochemical conversion (fermentation and anaerobic digestion) are two main available  
54 technologies for biomass conversion into energy [10]. Biomass gasification converts solid  
55 carbonaceous biomass into gaseous fuels under controlled conditions with limited oxygen and  
56 produces a mixture of hot gases that are cleaned and can be utilized in power generation through  
57 gas turbine [11, 12]. The product gas of biomass gasification is considered most important due to  
58 direct use for power generation, but it requires suitable operating conditions and product gas  
59 cleaning strategies for final applications[13]. The producer gas holds; H<sub>2</sub>, CO, CO<sub>2</sub>, CH<sub>4</sub>, N<sub>2</sub>, water  
60 vapours and other types of impurities i.e. alkali compounds, chlorine, sulphur, tar, nitrogen, char  
61 and particulates [14]. Syngas (CO+H<sub>2</sub>) produced during biomass gasification is an eco-friendly  
62 fuel for electricity generation and considered a versatile technology [15]. Hydrogen gas is an  
63 efficient clean energy carrier for the production of electricity that can be produced from biomass  
64 gasification. CH<sub>4</sub> and other liquid fuels can also be generated from syngas [1].

65  
66 Many researchers have reported the studies on the effect of gasifier type, the composition of bed  
67 material, gasification temperature, equivalent ratio (ER), biomass feedstock type on the  
68 gasification and product gas composition [16]. A variety of designs and technologies were  
69 developed in combustion plants, gasifiers, and pyrolysis plants. Fixed bed gasifiers and fluidized  
70 bed gasifiers technologies were largely investigated for biomass gasification by a number of  
71 scientists in past decades [17]. The disadvantage of the fixed bed gasifiers is the difficulty in

72 maintenance of the constant operational temperature [16]. Furthermore, the bubbling fluidized bed  
73 biomass gasification is largely preferred over other technologies because of high conversion  
74 efficiency, uniform temperature profile in the reactor that is suitable for gas-solid interactions.

75  
76 Karmakar et al. [18] have studied the rice husk gasification in FBG to examine the influence of  
77 temperature variation from 650–725°C with air as a gasifying medium at 0.25 ER. Their results  
78 suggested that with temperature increment, H<sub>2</sub> and CO were increased in the range of 17.22–  
79 18.49% and 24.89–26.59%, while CO<sub>2</sub> and CH<sub>4</sub> were decreased from 14.92–12.61% and 2.62–  
80 1.96%. The improvement in CCE from 71.51–75.82% with temperature was due to high  
81 conversion of unburned particles at high temperatures. The study of Subbaiah et al. [19] explored  
82 the gasification potential of groundnut shell (GNS) in FBG in 650–900 °C at 0.20 to 0.40 ER. They  
83 investigate the air-steam gasification that suggested the gas yield of CO and H<sub>2</sub> was increased with  
84 a rise in temperature and maximum CCE was 83.4% at 800 °C. The maximum HHV (6.9 MJ/Nm<sup>3</sup>)  
85 was observed at 0.30 ER and 800 °C temperature.

86  
87 Singh et al. [19] reported the gasification process of ground Nutshell (GNS) at 0.29–0.33 ER. The  
88 gasification temperature was 650–800 °C while air was used as a gasifying agent. They used  
89 conventional charcoal in bed heating. The most optimum ER reported for GNS gasification was  
90 0.31 that was showed 5.74% of CH<sub>4</sub>, 91% of CCE and 71.8% of CGE. Both the above studies of  
91 GNS suggested the optimum ER's were in the range of 0.30–0.31 and Singh et al. [20] study  
92 reported highest CCE at 0.31 ER. Sarker et al. [21] reported the alfalfa pellets gasification in FBG  
93 that was found attractive fuel for grid power generation. They studied gasification at 0.25 and 0.30  
94 ER and their results demonstrated the increment in bed temperature with an increase in ER. In

95 addition, the CGE of 39% and the gas yield of 1.6 Nm<sup>3</sup>/kg was observed. The LHV of 4.2 MJ/Nm<sup>3</sup>  
96 was obtained that indicate the alfalfa is promising biomass in terms of energy conversion. Most of  
97 the experimental parameters were enhanced by increasing the input air at a constant feed rate.

98  
99 Maglinao Jr. et al. [22] analysed the CCE, heating values and gasification efficiencies of three  
100 feedstock high tonnage sorghum, beef cattle manure and cotton gin trash in BFG in the temperature  
101 range of 730–790 °C and ER (0.3–0.5). They observed high carbon content and high efficiencies  
102 for tonnage sorghum. The optimum H<sub>2</sub> generation was found at 780 °C and 0.40 ER. The steam,  
103 as well as air gasification of sawdust, was performed to investigate the thermodynamic effect. Air  
104 was proven as an efficient gasifying agent that showed higher energy efficiency than steam  
105 gasification. The efficiency was continuously decreased by increasing ER when either steam and  
106 air used as a gasifying medium [23]. The product gas composition of rice husk gasification in a  
107 BFBG has been investigated previously, the composition of H<sub>2</sub>, CH<sub>4</sub>, and CO was decreased with  
108 an increase in ER, but the composition of CO<sub>2</sub> was increased. The appropriate ER value reported  
109 for its gasification was 0.2–0.3. [24]. Mohammed et al. [25] performed gasification in FBG using  
110 empty fruit bunch (EFB) as biomass and air as a gasifying agent in the temperature range of 700–  
111 1000 °C. The H<sub>2</sub> and CH<sub>4</sub> concentrations were increased from 10.27 to 38.02 and 5.84 to 14.72 %  
112 respectively with increasing temperature. The concentration of CO was increased from 21.87–  
113 36.36%, while the concentration of CO<sub>2</sub> decreased from 63–12%. The gas yield was reached to  
114 ~92% at 1000 °C.

115  
116 Sciazko et al. [26] reported that air gasification is mostly performed in 726–926 °C temperature  
117 range in FBGs, while during air-steam gasification the increase in hydrogen generation, increased

118 the produced syngas with a high calorific value that helps to decrease the mixing of hydrocarbon  
119 and tar. High molecule weight tar components were observed at high temperature in 100 kW dual  
120 fluidized bed gasifier (DFBG). The tar molecules were primarily treated within gasifier and  
121 secondary treatment was outside the gasifier by different techniques; baffled filters, rotating  
122 particle separators, fabric filters, electrostatic filters, ceramic filters, and scrubbers etc. [27]. The  
123 torrefaction effect on syngas quality of SRC chips was investigated in BFBG. Syngas quality was  
124 investigated by tar concentration and gas yield. About 47% reduction in tar yield has been reported  
125 from BFB gasification of SRC with steam and air as a gasifying medium [28]. Another attempt  
126 was made when SRC willow gasification was tried in a down-draft gasifier but results showed that  
127 willow chips were not gasified due to bridging within the hopper. Afterwards, a stirring bar was  
128 employed to prevent bridging and gasification was done successfully. The product gas collection  
129 was unsuccessful, therefore could not be further analyzed [29].

130

131 To the best of our knowledge, there is limited information available on short rotation coppice  
132 gasification in BFBG. Therefore, this study is designed to fill the gap in knowledge concerning  
133 the gasification of SRC willow woodchips and thermochemical assessment. Detailed  
134 thermogravimetric analysis and effect of different operating variables such as ER and temperature  
135 on product gas compositions of SRC gasification are studied. SRC willow chips were selected due  
136 to resprouting capacity after coppice, ease of harvesting, ease of propagation, broad genetic  
137 breeding and high yield, which is able to fulfil the energy demands by high power generation [30].  
138 The single planting of SRC can be harvested more than seven times due to resprouting ability [31].  
139 The experiments were performed to investigate SRC gasification in a BFBG using air as a  
140 gasifying agent focusing on temperature profiles and product gas composition under different

141 parameters. The biomass degradation behaviour was examined by TG/DTG to estimate the heat  
142 flow and decomposition characteristics of biomass. In addition, the effect of ER on temperature  
143 was studied to explore exothermic and endothermic reaction during gasification. The HHV, LHV,  
144 CGE and CCE were calculated to examine the performance of gasifier. This is a comprehensive  
145 study that discloses the optimum and best operating conditions for SRC willow gasification in a  
146 bubbling fluidized bed gasifier. Furthermore, this study also covers the detailed product gas  
147 composition analyses to examine the SRC gasification and gasifier performance evaluation.

## 148 **2 Experimental**

### 149 **2.1 Biomass characteristics**

150 SRC willow woodchips (size: 3–10 mm) from a local SRC willow grower were selected for  
151 gasification in bubbling fluidized bed biomass gasifier (BFBBG). The proximate and ultimate  
152 analysis of SRC willow woodchips was performed using TGA Q500 and is given in Table 1 [7,  
153 32]. The TGA/DTG analysis was done to determine the thermal behaviour and degradation  
154 characteristics of biomass [33]. The TGA/DSC analysis was performed to examine the heat flow  
155 per unit mass with temperature under an air atmosphere. The comparison of burning profiles of  
156 TG/DTG and TG/DSC was used to determine the stages of thermal degradation of biomass [34].

### 157 **2.2 Experimental setup of Gasifier**

158 The bubbling fluidized bed biomass gasifier (BFBBG) is schematically represented in Fig. 1  
159 consists of a biomass feeding hopper, screw feeder, fluidized bed gasification reactor, cyclone, gas  
160 cooling unit, tar removal unit (a mop fan unit, a biomass/ char bed), electrically heated combustor,  
161 an air supply/ preheating system and data acquisition devices. In BFBBG, the gasifying reactor can  
162 be virtually divided into the bed (gas-solid reaction) zone and the freeboard (gas phase reaction)

163 zone. The bubble formation within the bed of bubbling fluidized bed biomass gasifier increased  
164 the heat transfer rate of bed material and mixing efficiency of fuel particles and gasifying agent.  
165 The main gasifier consists of a stainless-steel reactor had dimensions of 108 mm diameter and  
166 height of 1800 mm. The fluidization air was entered through a blower. The flow rate of air was  
167 controlled by a rotameter. The air was fed into gasifier reactor by an air distribution plate with a  
168 pore size of 100  $\mu\text{m}$  and thickness of 10 mm which also allows preheating up to required  
169 gasification temperature (700–900  $^{\circ}\text{C}$ ) through electric pre-heater [35].

170

171 The SRC willow woodchips were fed into the combustor by a screw feeder just above the air  
172 distribution plate. The biomass feeding unit supported the desired feed rate of woodchips by using  
173 a screw auger and timed stirrer. The auger is used to transfer woodchips from the hopper into the  
174 reactor by an inverter. The inverter was used to control the frequency of the feeder motor. To  
175 prevent from backflow of biomass and sand particle into the feeding unit, a small amount of air  
176 was also introduced through feeder hopper. The temperature profiles of the gasification reactor  
177 were continuously monitored by placing eight K-type thermocouples at different distances from  
178 the distribution plate. These thermocouples are labelled as T1, T2, T3, T4 (bottom and middle  
179 thermocouples) and T5, T6, T7 and T8 (upper thermocouples) which are located at -5, 9, 17, 25,  
180 45, 74, 105 and 150 cm height above from the distribution plate. T1 was located in the air chamber  
181 under the distribution plate, while T2–T5 measures the gasification temperature variation  
182 occurring in dense bed zone and T6–T8 are uppermost thermocouples set at freeboard region of  
183 reactor, monitoring the temperature variation of the gas exit.

184



185 The reactor was equipped with pressure sensors at different heights to examine the fluidization  
186 conditions of the bed. The bubble formation, rising and bursting of bed material in the reactor was  
187 observed by increasing the fluidization air flow rate that is shown in Fig. 2. The gas particles  
188 usually move upward from bed at a minimum fluidization velocity that is less than 5 m/s. The  
189 rising of gas from bed create bubbles that maintain bubble emulsion and fluidization state at the  
190 bed. After this dense bed, a freeboard region is present that reduces the supercritical velocity and  
191 return the particles towards the bed region. In this way, bed material almost remains fixed [36].  
192 The pressure difference is closely checked at dense bed region and freeboard region to detect any  
193 sign of defluidization and agglomeration during gasification. If an abrupt change in pressure  
194 difference recorded across dense bed region and reactor temperature, it means defluidization.

195  
196 This research was designed to focus on product gas composition and temperature profiles. All the  
197 above mentioned tests were performed to avoid defluidization and agglomeration during  
198 gasification [37, 38]. At the exit point of the reactor, a cyclone is fitted for the removal of particles  
199 from product gas to achieve high efficiency. The ash particles are collected in an ash pot from the  
200 bottom of the cyclone. After cooling, product gas by gas cooler it is introduced into the mop fan  
201 cleaning unit. The centrifugal fan casing mop with 70 mm fibre length and 0.4–0.6 mm diameter  
202 of each fibre is used for gas circulation, de-dusting of contaminated product gas stream and  
203 efficient removal of gaseous contaminants. The efficiency of particles removal is improved by a  
204 water spray, fibre number and fibre arrangement. An on-line gas analyzer (ABB Easy Line  
205 analyzer) is fitted at the end of a gasifier to continuously determine the product gas (CO, CO<sub>2</sub>, CH<sub>4</sub>  
206 and H<sub>2</sub>) composition. The analyzer calibration was done with standard gas samples. For  
207 comparison, the product gas was also analyzed in an off-line offline gas chromatography (GC)

208 analyser. All of the measured and processed data such as product gas profile and temperature are  
209 continuously monitored by computerized systems.

### 210 **2.3 Gasifier operating conditions**

211 The operational parameters of gasifier and gasification process are characterized by equivalence  
212 ratio, temperature profile along with the height of the reactor, feeding rate and gas concentrations  
213 at the exit. The constant biomass flow rate was achieved through repeated calibration after regular  
214 intervals by checking the amount of biomass flow from the hopper to the gasification reactor in a  
215 specific time through the auger. The timed stirrer was adjusted as 5 sec/min to the hopper. Timed  
216 stirrer and feeder confirmed the stable feed rate to achieve steady product gas and temperature  
217 profile. An auto stirrer was used to stirrer the biomass constantly to prevent bridging and to  
218 improving the gas quality [39]. The reliable sampling for reproducible results of product gas  
219 analysis was obtained by using different rotation speed of auger i.e., 10, 11 and 12.5 Hz. The auger  
220 speed controls the feeding rate of wood chips. The inverter of gear motor controls the auger  
221 rotational speed.

222  
223 The gasification was performed at three different ERs; 0.25, 0.29 and 0.32 in BFBG. The  
224 fluidization and gasification process are examined by a set of thermocouples and pressure sensors.  
225 Compressed air was used as a fluidization medium at room temperature. The operating conditions  
226 for biomass gasification of willow chips are given in Table 2. When desired temperatures have  
227 obtained in the gasification reactor, the biomass is introduced into the gasifier and air was fed  
228 accordingly to the selected ER values. A small amount of air (3 L/min) at room temperature and 1  
229 atm pressure was introduced into the hopper to prevent any backward diffusion of biomass and  
230 sand particles. The ER was modified by adjusting the gasification airflow rats; 45, 65 and 80 L/min

231 for 0.25, 0.29 and 0.32 respectively. After gasification initiation, a steady state condition was  
 232 achieved in the reactor after about 30 min of feeding and all variables were continuously  
 233 monitored. All parameters in the rig (pressure, temperature and product gas composition analysis)  
 234 were recorded by the data acquisition system.

## 235 **2.4 Estimation of Gasifier's performance**

236 The performance of BFBG was investigated by calculating gas yield, cold gas efficiency (CGE),  
 237 Carbon conversion efficiency (CCE), high heating value (HHV) and low heating value (LHV) of  
 238 product gas. The gasifier performance was monitored by comparing the gasification process at  
 239 different ERs (0.25, 0.29 and 0.32). These calculations were performed by using following  
 240 equations 1–5 [6, 21].

241 a. HHV

$$242 \text{ HHV} = (\text{H}_2 \text{ conc. in product gas} * \text{HHV of H}_2) + (\text{CO conc. in product gas} + \text{HHV of CO}) + (\text{CH}_4 \\ 243 \text{ conc. in product gas} * \text{HHV CH}_4) \quad (1)$$

244 b. LHV

$$245 \text{ LHV}_{\text{gas}} = \sum V_i * \text{LHV}_i \quad (2)$$

246 where  $V_i$  = % composition of gas component in the product gas

247  $\text{LHV}_i$  = lower heating value of the individual gas component

248 c. Gas yield

$$249 \text{ Total gas yield} = \text{Amount of N}_2 \text{ fed to the gasifier} * \text{N}_2 \text{ concentration in the product gas} \\ 250 = \text{N}_2 \text{ (m}^3\text{/h)} * (100 - \sum V_{\text{gi}}) \quad (3)$$

251 where  $V_{\text{gi}} = \text{N}_2 = \text{Air fed into the gasifier (m}^3\text{/h)} * \text{N}_2 \text{ concentration in product gas}$

252 d. Cold gas efficiency

253 Cold gas efficiency was calculated by the following equation:

$$254 \text{ CGE}(\eta) = \frac{\text{Gas yield} * \text{LHV}_{\text{gas}}}{\text{Biomass feeding rate} * \text{LHV}_{\text{biomass}}} * 100 \quad (4)$$

255 e. Carbon conversion efficiency

256 
$$\text{CCE}(\%) = \frac{12(\text{CO}_2 + \text{CO} + \text{CH}_4 + 2.5\text{CnHm}) * \text{Gas yield} * 100\%}{22.4 * 298 / 273} \quad (5)$$

257

## 258 **3 Results and discussion**

### 259 **3.1 Thermogravimetric analysis**

260 The Thermogravimetric analysis (TGA) was performed to investigate the chemical reactions and  
261 thermal stability of biomass with quantitative measurement of weight loss over a specific  
262 temperature range. Fig. 3 shows the sample weight loss and derivative mass loss with temperature  
263 by using air as a reacting medium. Blue curve indicated four degradation stages; drying,  
264 devolatilization, char combustion and ash formation [40]. Red line shows the DTG curve. The  
265 initial mass loss (up to ~9%) was observed in the drying stage at temperatures of 26–125 °C that  
266 is associated with the removal of moisture. SRC willow chips showed 10% moisture content that  
267 was determined by ultimate analysis as given in Table 1. This moisture content is most suitable  
268 for gasification. The presence of higher moisture content needs more energy for the drying process  
269 during gasification [41].

270

271 Most of the volatile components, tar, gases and char produced during thermal decomposition of  
272 biomass (devolatilization) and almost 70% mass loss of initial weight occurred in devolatilization  
273 zone (126–363 °C) region [33]. The ignition temperature ( $T_{\text{ign}}$ ) represents the onset of  
274 devolatilization stage and known as an active pyrolysis region, which was started at 259 °C. The  
275 peak temperature of the devolatilization region was 337 °C that is known as glass transition  
276 temperature ( $T_g$ ) as derived from TGA/DTG curves [42]. The mass loss of ~27% was observed in

277 the temperature region of 363–513 °C because of char combustion. Finally, the ash formation was  
278 observed in the temperature range of 513–850 °C containing ~1% biomass sample.

279  
280 The DTG curves showed two peaks; first sharp and strong peak was observed in 261–374 °C  
281 temperature range having a maximum rate of mass loss 35 %/min at 338 °C. This region revealed  
282 the degradation of carbon content and devolatilization of biomass. The second peak in the DTG  
283 curve indicates the char combustion that was obtained in the secondary pyrolysis zone (275–510  
284 °C) with maximum mass loss rate ~11 %/min at 483 °C. Beyond 510 °C, the DTG curve showed  
285 a slow rate of mass loss ~1 %/min because degradation is almost completed in this region and only  
286 char residue left behind. Thermal degradation behaviour of biomass showed that pyrolysis of  
287 hemicellulose usually occurred at a temperature below than 350 °C. While cellulose pyrolysis  
288 occurred in temperature ranges 250–500 °C. There was no sharp peak beyond 500 °C because most  
289 of the biomass have already degraded and only lignin shows some thermal stability [34, 42, 43].  
290 Nyakuma et al. [44] studied thermochemical assessment of the empty fruit bunch (EFB) by heating  
291 in the temperature range of 50 °C to 900 °C at 10°C/min heating rate. TGA results suggested four  
292 stages of biomass thermal decomposition and 70% weight loss was observed in devolatilization  
293 stage at 325 °C peak temperature.

### 294 **3.2 Differential scanning calorimetry**

295 Fig. 4 shows TG/DSC curve heat depicted the heat flow per unit mass during exothermic and  
296 endothermic reactions with temperature variation. The main reactions that take place during  
297 biomass gasification are given in Table 3. In accordance with Le Chaetlier's principle, endothermic  
298 products and exothermic reactants are favoured at high temperature. At initial, drying and heating

299 of biomass require heat and endothermic reactions are favoured. Two sharp peaks were observed  
300 in the temperature range of 315–500 °C which showed the exothermic reaction of gasification.

301  
302 Most of partial char combustion and devolatilization occurs in this region, which releases a large  
303 amount of heat due to the combustion of unburned particles and release of volatiles. At this stage,  
304 TGA also confirmed the breakdown of larger chains of hydrocarbon into smaller chains, and  
305 thermal decomposition of fuel into the gaseous product [34]. The heat flow curve suggested that  
306 as the gasification proceeds with the rise of temperature, endothermic reactions such as Boudourad  
307 reaction, water gas shift reaction and methane reforming reaction were favoured. The gas products  
308 are then reformed through these reactions [45]. Zhao et al., [46] reported the detail pyrolysis of  
309 corn straw and soybean straw with TG/DTG and TG/DSC analysis in a fixed bed reactor. Their  
310 results found four pyrolysis stages and temperature increased with increasing heat rate that  
311 produces high char yield.

### 312 **3.3 Effect of ER on gasifier temperature**

313 The temperature of gasification is considered important in determining the composition and yield  
314 of the product gas. Temperature is not an independent factor in gasification. The temperature  
315 profile of gasifier is linked to the amount of air available (ER), therefore, both are considered  
316 important parameters for gasification. The temperature profiles of gasifier are controlled by ER;  
317 with an increase in ER the amount of air introduced into the reactor is also increased which  
318 enhances the oxidation rate of biomass. This enhanced oxidation rate increases the heat release  
319 and carbon conversion content which results in an increment in the temperature of gasifier reactor.  
320 Fig. 5 presents the influence of ER on the temperature profiles of the gasifier reactor (T2–T8). By  
321 increasing ER from 0.25 to 0.32, the temperature distribution in all regions such as; dense board

322 and freeboard showed an increase to their maximum values of 817, 812, 785, 777, 778, 782, 548  
323 °C for T2 to T8 respectively. Therefore, higher ER value showed that most of the partial  
324 combustion occurs in the gasifier reactor due to increased temperature.

325  
326 This increasing temperature with ER also continued distinctive differences between all sensors at  
327 a different height. This increment in temperature was due to more air entered into the reactor in  
328 oxidation zone and promote combustion that has increased the temperature of gasifier [21]. The  
329 results indicated that when ER is increased from 0.25 to 0.29 then 0.32, the temperatures at all  
330 thermocouple in the reactor were smoothly increased. As the high temperature is achieved in the  
331 gasifier, a series of endothermic reactions including drying, char combustion with exothermic  
332 reactions (devolatilization) started which describe the temperature behaviour along with the height  
333 of the reactor. At the exit of the gasifier reactor, the temperature is decreased because of heat losses  
334 and endothermic char combustion and tar cracking [47]. This trend is also confirmed by the heat  
335 flow curve shown in Fig. 4. Nevertheless, there is a decrease in temperature at -5 cm distance (T1)  
336 from the distribution plate because of introducing an additional air without preheating into the  
337 reactor. [48]. The highest temperature observed in the oxidation zone while the lowest temperature  
338 was recorded in the upper portion of gasifier in the pyrolysis region [49]. The high temperature  
339 favoured water gas shift reactions which further promote steam methane reforming reaction [50].  
340 By comparing the effect of different ER value, the higher temperature was observed with ER=0.32  
341 which indicate the increase in temperature by increasing ER value.

342  
343 Temperature is considered the most important factor that affects the gasification process.  
344 González-Vázquez et al., [51] estimated the effect of temperature on pine kernel shell gasification,

345 product gas concentrations, gas yield and CGE. The results concluded that the rise in temperature  
346 from 700 to 900 °C favoured high H<sub>2</sub> production and best gasifier performance. From literature, it  
347 is observed that higher temperature is responsible for higher hydrogen concentration and low tar  
348 content because of thermal tar cracking reactions. Due to this more volatiles were released at high  
349 temperature and increased the overall gas yield. The BFBG is considered a promising option for  
350 hydrogen generation. Therefore, hydrogen generation through thermochemical route such as  
351 biomass gasification in BFBG is remarkable technology. The desired gasification temperature is  
352 achieved by partial combustion. The yield of producer gas, CGE and tar contents in the syngas are  
353 dependent on the temperature of gasification [52]. Perez et al. [53] investigated the thermodynamic  
354 and fluid-dynamic analysis of sugarcane bagasse in BFBG. Geldart's types of particles were used  
355 to examine the fluidization parameter in gasification. The results showed the 4.56 MJ/Nm<sup>3</sup> of LHV  
356 and 0.8–1.21 mm of ideal particle size was suggested for large scale gasification.

357

### 358 **3.4 Effect of equivalence ratio on product gas compositions**

359 The equivalence ratio (ER) has a greater effect on concentrations of product gas and calorific value  
360 of syngas that directly affects the performance parameters of gasification [15]. The ER was varied  
361 from 0.25 to 0.32 to examine the effect of ER on product gas composition. The gasification airflow  
362 rate was changed from 45 to 65 and then 80 L/min to obtain a selected range of ER in the gasifier.  
363 These experiments were performed with feeding rates 1920.9, 2126.8 and 2469.6 g/h for 0.32, 0.29  
364 and 0.25 ER respectively. The stable and constant biomass feeding is used for biomass gasification  
365 because it is considered important for reliable product gas sampling and their analysis. The feeding  
366 process and product gases are affected by moisture content, auger rotational speed, dimensions of



367 biomass particle. The size of SRC willow was 3–10 mm that provides excellent heat transfer rate  
368 [54, 55].

### 369 **3.4.1 Online analysis of product gas compositions**

370 ER values distinguish the combustion and gasification process. ER value less than 1 is considered  
371 for gasification and optimum range from 0.2–0.4 has been reported for biomass gasification. If ER  
372 value is taken below 0.2 then it produces unnecessary char, syngas with low heating value and  
373 incomplete gasification occurred. While ER values above 0.4 also cause a problem, such as  
374 extreme production of combustion products (CO<sub>2</sub>, H<sub>2</sub>O) [50]. The product gas found from air  
375 gasification of biomass is usually composed of some combustible and incombustible gases. The  
376 analysis of these products (CO, CO<sub>2</sub>, CH<sub>4</sub>, and H<sub>2</sub>) was done by online gas analyzers. Four runs of  
377 gasification were performed at each ER value to check the repeatability and reliability of the  
378 experiments and product gas values. Fig. 6 gives the distribution of product gas composition at  
379 various ERs monitored by the on-line gas analyzer as well as GC analyzer. Only slight differences  
380 in product gas composition were observed for each run, which confirmed the reliability and  
381 reproducibility of the experiments.

382

383 The product gas concentrations with online gas analyzer are presented in Table 4. At 0.25 ER, the  
384 average concentrations of CO, CO<sub>2</sub>, CH<sub>4</sub> and H<sub>2</sub> were 16.98, 17.49, 4.43 and 9.95% respectively.  
385 The concentrations observed at 0.29 ER were 14.20, 18.19, 3.94 and 8.26 % for CO, CO<sub>2</sub>, CH<sub>4</sub>  
386 and H<sub>2</sub> respectively. While the compositions of product gas at ER 0.32 were 12.72, 19.21, 3.88  
387 and 6.30% for CO, CO<sub>2</sub>, CH<sub>4</sub> and H<sub>2</sub> respectively [56]. These values show that with increasing ER  
388 value from 0.25 to 0.32, the concentration of CO, CH<sub>4</sub>, H<sub>2</sub> decreased while CO<sub>2</sub> increased. The  
389 product gas composition obtained from Fig. 6(a-c) indicates that the concentration of CO

390 decreased from 16.98 to 12.72% with an increment in ER from 0.25 to 0.32. The concentrations  
391 of CH<sub>4</sub> and H<sub>2</sub> were also decreased from 4.43–3.88 % and 9.95–6.30% respectively by increasing  
392 ER in the selected range. The decrease in H<sub>2</sub> concentration was observed because of the water gas  
393 shift reaction in which H<sub>2</sub> consumption rate was greater as compared to H<sub>2</sub> formation rate [56].  
394 While the decreased concentration of CH<sub>4</sub> from 3–4% with increasing ER was due to methanation.  
395  
396 However, the CO<sub>2</sub> composition was found to increase from 17.49 to 19.21% by increasing ER  
397 from 0.25 to 0.32. By increasing ER, more air entered into the reactor, CO and CH<sub>4</sub> were burned  
398 with O<sub>2</sub> and formed CO<sub>2</sub> due to excessive availability of air. The results of CO, H<sub>2</sub> and CH<sub>4</sub>  
399 compositions displayed opposite trend to CO<sub>2</sub> composition in product gas profile of gasification.  
400 These trends were due to different ER values because ER indicates the quantity of actual air  
401 available for volatile formation and gasification of fuel. During gasification, gas products react  
402 with oxygen and produce CO, CH<sub>4</sub>, H<sub>2</sub> and CO<sub>2</sub> gases. These gaseous products are formed by  
403 series of reaction including carbon reaction, Boudouard reaction, water gas shift reaction or  
404 methanation reactions as already depicted in Table 3 [52].  
405  
406 Therefore, low concentration of combustible gases (CO, CH<sub>4</sub> and H<sub>2</sub>) was found at high ER value  
407 and diminished the product gas quality. The low ER favoured endothermic reactions that are char  
408 + CO<sub>2</sub> and water gas shift reactions. Therefore, more char and CO<sub>2</sub> used in these reactions which  
409 lower the CO<sub>2</sub> composition [57]. Considering the trends of gas concentrations with decreasing ER,  
410 the maximum increment is obtained for CO concentration while the small increment is found in  
411 CH<sub>4</sub> concentration. The increment in H<sub>2</sub> concentration is seen smaller than the increment in CO  
412 concentration. Likewise, the increment in CO concentration is greater than the decrease in CO<sub>2</sub>

413 concentration with decreasing ER. Similar results were reported by Sarker et al. [21] which showed  
414 the increase in CO<sub>2</sub> concentration when the ER value was increased from 0.20–0.35.

415

416 Though, the current study showed enhanced CH<sub>4</sub> concentration nearly 4–3%, which is greater than  
417 CH<sub>4</sub> concentration (2.6–2.0%) of wheat straw pellet gasification as reported Sarker et al. [21].  
418 Kim, Yang et al. [48] reported that a decrease in the concentration of H<sub>2</sub> and CO was due to water  
419 gas shift reaction. By increasing ER from 0.25 to 0.32, the H<sub>2</sub> product gas was decreased by  
420 approximately 9–6% due to the dominant oxidation reaction at higher ER value because oxidation  
421 in gasification reactor dominates and produce less H<sub>2</sub> gas [58]. The higher concentration of CO in  
422 the product gas was also reported by Makwana, Joshi et al. [59] which was due to the lower value  
423 of ER. They gasified rice husk and char of rice husk by varying the ER from 0.30 to 0.38. The  
424 higher CO (18%) and H<sub>2</sub> (5.6%) composition were found at low ER due to endothermic steam  
425 reforming reaction. In the present study, the gasifying medium was air which increased oxidation  
426 reaction by producing CO<sub>2</sub> from the utilization of CO and O<sub>2</sub>. The air also promotes complete  
427 oxidation of fixed carbon component and oxygen resulting CO concentration drops. More residual  
428 carbon is produced by increasing gasifying medium and combustion due to pyrolysis in steam  
429 gasification which increases the carbon conversion efficiency.

### 430 **3.4.2 Gas chromatography analysis of product gas composition**

431 The product gas composition analysis was also carried out through Gas chromatography (GC), to  
432 check the reliability and reproducibility of the online gas analyzer. When all gasification  
433 parameters become stable, the four sampling bags of 0.5 litre were filled with product gas for  
434 offline GC analysis. This analysis was performed with the same ER's as used for online analysis.  
435 The composition of product gas measured at the inlet of combustor was comprised of CO<sub>2</sub>, CO,

436 H<sub>2</sub>, CH<sub>4</sub> and a small amount of O<sub>2</sub>. This gas composition was important for partial oxidation. Table  
437 4 shows GC analysis of product gas compositions at different ERs.

438

439 The GC analysis showed 16.64, 17.99, 4.67, 8.96% concentrations of CO, CO<sub>2</sub>, CH<sub>4</sub> and H<sub>2</sub>  
440 respectively at 0.25 ER. Karatas, Akgun et al. [52] reported pilot-scale gasification of natural wood  
441 at the same ER 0.25 as reported by the present designed study. They reported the 5% concentration  
442 of CH<sub>4</sub> that is nearly similar to the current study of SRC at this ER. The concentrations observed  
443 at 0.29 ER were 14.50, 18.16, 4.06 and 8.31% for CO, CO<sub>2</sub>, CH<sub>4</sub> and H<sub>2</sub> respectively. While the  
444 compositions of product gas at ER 0.32 were 12.29, 18.24, 4.22 and 6.53% for CO, CO<sub>2</sub>, CH<sub>4</sub> and  
445 H<sub>2</sub> respectively [56]. The results of product gas concentration by GC analysis are in clear  
446 agreement with the online analyser. The GC analysis results showed that CO<sub>2</sub> increased from 17.99  
447 to 18.24% with increasing ER (0.25–0.32). This is because the oxygen supply was dominant as of  
448 increasing air feeding that burns volatile component of biomass by producing more CO<sub>2</sub>. This gas  
449 also dilutes the other combustible gases therefore, at higher ER less concentration of H<sub>2</sub>, CH<sub>4</sub>, and  
450 CO is produced. At 0.32 ER, the concentration of CH<sub>4</sub> was low (4.22%) but it can significantly  
451 change the gas heating values [60].

452

453 The product gas composition results of online analyses and off-line GC analysis are already given  
454 in Table 4. The results of product gas obtained from both analyzers are then compared to check  
455 the efficiency of analyzers. The comparison of product gas profile at 0.25 ER is shown in Fig. 6(a).  
456 Their results showed the one-factor difference in H<sub>2</sub> concentration of GC and online analysis. The  
457 H<sub>2</sub> concentration recorded by GC analyser was 8.96%, but online analyser recorded 9.95%, that is  
458 marginally different. However, all other remaining product gas composition showed stability from

459 both analyses [50, 57]. The comparison of product gas at 0.29 ER is represented in Fig. 6(b). The  
460 results indicated a slight difference in CH<sub>4</sub> composition. The CH<sub>4</sub> concentration recorded by GC  
461 analyser was 4.06%, however, online analyser recorded 3.94%. While the other gas compositions  
462 were almost the same from both analysers. At ER 0.32, a comparison of product gas profiles from  
463 GC and online analyzers is given in Fig. 6(c).

464

465 The comparison confirmed the quantitative composition of product gases that shows only one  
466 factor difference in CO<sub>2</sub> concentration while other gas compositions almost same and showed  
467 uniformity from both analysers. This comparison was effective and confirmed the efficiency of  
468 both analysers. Therefore, the qualitative and quantitative results of product gas at different ER  
469 from both GC and online analysers are in excellent agreement with each other and confirmed the  
470 efficiency of analysers and the energy profile of SRC willow.

### 471 **3.5 Gasifier performance evaluation**

472 The performance of bubbling fluidized bed gasifier was examined in terms of product gas  
473 concentrations and carbon conversion. A set of desirable efficiency parameters were investigated  
474 to check the efficiency of converting input mass into synthesis gas product with reduction of tar.

#### 475 **3.5.1 Bed temperature and tar yield**

476 The effect of ER on average bed temperature and tar yield was studied. Fig. 7 confirms that ER  
477 values have a positive linear correlation with average bed temperature and negative linear  
478 correlation with tar yield. When the bed temperature increased from 776 to 817 °C, a decrease in  
479 tar yield from 16.78 to 7.24 g/m<sup>3</sup> by was noticed by increasing ER from 0.25 to 0.32 respectively.  
480 Therefore, the increment in the ER in the gasifier enhanced the average bed temperature about ~40

481 °C, which is considered effective for gasification. This increment in bed temperature with ER was  
482 due to more air availability for oxidation reaction that promotes heat release.

483

484 The high bed temperature also favoured H<sub>2</sub> and CO concentration in accordance with Le  
485 Chatelier's principle, which depicted that reactant substance in exothermic reactions and product  
486 substance in endothermic reactions favoured at a higher temperature. Therefore, endothermic  
487 steam gasification reaction is strengthened at a higher temperature with increasing ER [18]. The  
488 increase in bed temperature with ER was also due to the uniform size of bed particles, which was  
489 easily deposited on the bed surface. These particles were burnt easily when coming in contact with  
490 bed surface and release heat. Air can easily circulate throughout the reactor due to pressure  
491 fluctuation in the reactor and bed surface that improved fluidization and combustion behaviour  
492 and increased the bed temperature [20]. Improper fluidization may cause agglomeration and failure  
493 of the gasification process [38]

494

495 The increase in carbon conversion efficiency and bed temperature with the increase of ER from  
496 0.25 to 0.32 improves the tar decomposition. This is because of thermal cracking and reforming  
497 reactions [50]. ER played an important role in tar content and their properties. By increasing ER  
498 from 0.25 to 0.32, air availability is increased which decreased the tar yield from 16.78 to 7.24  
499 g/m<sup>3</sup> as given in Fig. 7. This decreasing trend was due to more combustion of hydrocarbons and  
500 tar cracking reaction at high ER. The tar cracking reactions including steam gasification reaction  
501 as well as reforming reaction decrease the tar yield. The partial combustion reaction increased the  
502 temperature of the reactor, which favoured char gasification with high conversion rate and reduces

503 the tar yield [37]. However, higher ER improves the bed temperature that causes tar decomposition  
504 and decreased the tar yield and this reduction in tar yield is very important for gasification.

### 505 **3.5.2 Evaluation of LHV and gas yield**

506 The gasification parameters such as LHV, Cold gas efficiency (CGE) and gas yield were  
507 investigated to examine the gasifier performance efficiency. The CGE is the percentage of LHV  
508 of biomass converted into LHV of product gas. CGE is also called gasification efficiency. As the  
509 ER value is varied from 0.25 to 0.32, all gasification parameters (gas yield, CGE, LHV, CCE)  
510 were also changed. Fig. 8 shows a decrease in LHV and an increase in the gas yield of product gas  
511 with increasing ER values. The LHV was decreased from 4.37 to 3.67 MJ/m<sup>3</sup> by increasing ER  
512 from 0.25 to 0.32. This was due to less production of combustible gases (CO and H<sub>2</sub>) which  
513 favoured a decrease in LHV. The LHV was decreased due to exothermic water gas shift reaction  
514 as well as dilution of syngas with air nitrogen [12]. The HHV was decreased from 4.70 to 3.95  
515 MJ/m<sup>3</sup> while the LHV was also decreased with increasing ER, this trend was also observed in the  
516 previous studies. Karatas, Akgun et al. [52] reported that the LHV of walnut shell and pistachio  
517 shell was decreased by increasing ER from 0.19 to 0.37. It can be seen in Fig. 8 that the gas yield  
518 increased from 3.93 to 4.55 m<sup>3</sup>/h by increasing ER from 0.25 to 0.32 respectively.

519  
520 The increment in gas yield is because of increment in the gasifying medium that is caused by  
521 increasing ER. That is the reason the gas yield is varied with a gasifying agent. The temperature  
522 becomes higher in oxidation zone at high ER, which favoured high volatilization of biomass and  
523 char gasification. Moreover, further increment in temperature, increase the gas yield due to the  
524 steam reforming reaction. Meng et al. [61] reported the sawdust gasification with different  
525 gasifying agents. The gas yield was changed from 2.11 to 2.41 m<sup>3</sup>/h with increment in the ER from

526 0.20–0.30. The amount of gas yield obtained in the present study is more than gas yield reported  
527 for sawdust. This increment in gas yield could be due to biomass type and operating conditions of  
528 gasifier but the overall trend of gas yield with ER is in accordance with the literature.

### 529 **3.5.3 Determination of CGE and CCE**

530 At the selected ERs 0.25, 0.29 and 0.32, the CGE varied from 49.63, 47.89 to 46.43% respectively  
531 also shown in Fig. 9. Cold gas efficiency was influenced by ER. CGE examines how much heating  
532 content of biomass is used to convert the feedstock into product gas. By increasing ER, the low  
533 heating value (LHV) of producer gas decreased because of excessive oxidation of feed and more  
534 inert nitrogen is also introduced with air which diminished the quality of product gas [62].  
535 Therefore, this rise in air availability diminished the product gas quality due to the large oxidation  
536 reaction of biomass.

537

538 The decreasing LHV of product gas showed the total energy conversion into product gas is  
539 decreased, which decreases the CGE [39]. Similar findings and trends of CGE and LHV with ER  
540 have been reported by Hamad, Radwan [63], Ahmed et al. [64] and Guo et al. [49]. The CCE is  
541 the percentage of gasified carbon content to the total carbon content in the added feed [18]. In an  
542 ideal system only, most of the biomass is to be transformed into desirable product gas mixture and  
543 other secondary particulates. However, in case of woodchips biomass gasification, carbon, oxygen  
544 and hydrogen in the feedstock are transformed into a mixture of synthesis gas, secondary products  
545 including carbon dioxide, methane and higher gaseous hydrocarbons and other unwanted  
546 particulates such as sulfur species, particulate matter and tars. The carbon conversion calculations  
547 at different biomass feeding rate were performed by using constant gasification airflow rate (44.72  
548 L/m) and during 60 min of feeding. The carbon conversion efficiency (CCE) was estimated at



549 0.32, 0.29, and 0.25 ER with 1920.9, 2126.8 and 2469.6 g/h feeding rates respectively, that is also  
550 displayed in Fig. 9.

551  
552 The results indicate that the highest carbon conversion (95.76%) was achieved with 1920.9 g/h  
553 feeding rate of biomass at 0.32 ER value. The CCE was 90.68 and 95.48% at 0.29 and 0.25 ER  
554 respectively. By increasing ER from 0.25 to 0.32, the CCE efficiency is varied from 95.48 to 95.76  
555 %. When ER is increased, more air is introduced into gasifier that favoured exothermic oxidation  
556 reaction. This exothermic reaction increased the temperature of the gasifier and also promotes the  
557 steam reformation that in turn increased the carbon conversion rate [50]. By increasing ER from  
558 0.25 to 0.32 more carbon content of the biomass was converted into product gas (CO, CO<sub>2</sub> and  
559 CH<sub>4</sub>) which leads to gradually increase in carbon conversion rate. Therefore, CCE reached its  
560 maximum value (95.76%) at 0.32 ER. Diyoke et al. [57] also reported that CCE depends on the  
561 rate of oxidation of carbon particulates Therefore, CCE is increased and CGE is reduced with  
562 increasing ER from 0.25 to 0.32.

## 563 **4 Conclusions**

564 In this present study, gasification characteristics of SRC willow chips were investigated using  
565 bubbling fluidized bed gasifier (BFBG) at 600–850 °C and at different equivalence ratios of 0.25,  
566 0.29 and 0.32. The thermochemical investigation was done by TG/DTG and TG/DSC analysis to  
567 explore the thermal stability and degradation characteristics of biomass. Furthermore, the influence  
568 of ER on concentrations of product gas was examined by online and offline analysis. The main  
569 findings of the study are summarized as follows:

- 570 • The TGA/DTG analysis was performed to examine the thermal degradation characteristics  
571 of biomass. The highest weight loss observed in the devolatilization stage was ~70% in the

572 temperature range between 126 and 363 °C. While two sharp peaks observed within the  
573 range of 315 to 500°C in TG/DSC curves indicate the exothermic reactions. Heat release  
574 can be utilized in power generation.

575 • By increasing ER, the temperature profiles of reactor increase and the highest temperature  
576 were observed in dense board region in the range of 650–850 °C. The increased bed  
577 temperature with increasing ER is considered important for tar reduction and to improve  
578 the carbon conversion rate.

579 • An increment in ER from 0.25 to 0.32, the GC and online analysis showed the average  
580 concentration of CO, CH<sub>4</sub> and H<sub>2</sub> decreased in the range of 16–12%, 4–3% and 9–6%  
581 respectively. In addition, the CO<sub>2</sub> concentration increased from 17–19 % in the product gas  
582 composition. This is because of more air availability for oxidation at high ER, which  
583 diminishes the product gas quality and lower the combustible gas concentrations. Both GC  
584 and online analysis of product gas compositions showed clear agreement with each other.

585 • Both the gas yield and CCE increased while LHV, CGE and tar yield gradually decreased  
586 with increasing ER from 0.25 to 0.32. The maximum carbon conversion efficiency of  
587 95.76% was observed at 0.32 ER. These parameters results confirmed the reliability of the  
588 gasification process, gasifier performance and product gas composition.

589 • TGA and gasification results showed the high thermal stability and high carbon conversion  
590 efficiency of selected SRC willow chips. Therefore, SRC willow biomass is recommended  
591 as renewable energy fuel for the future power generation industry and for the other  
592 applications.

593 **References**

594 1. Sikarwar, V.S., et al., An overview of advances in biomass gasification. *Energy &*  
595 *Environmental Science*, 2016. 9(10): p. 2939-2977.

596 2. Anupam, K., et al., Preparation, characterization and optimization for upgrading *Leucaena*  
597 *leucocephala* bark to biochar fuel with high energy yielding. *Energy*, 2016. 106: p. 743-  
598 756.

599 3. Williams, A., et al., Pollutants from the combustion of solid biomass fuels. *Progress in*  
600 *Energy and Combustion Science*, 2012. 38(2): p. 113-137.

601 4. Farzad, S., M.A. Mandegari, and J.F. Görgens, A critical review on biomass gasification,  
602 co-gasification, and their environmental assessments. *Biofuel Research Journal*, 2016.  
603 3(4): p. 483-495.

604 5. Sher, F., et al., Experimental investigation of woody and non-woody biomass combustion  
605 in a bubbling fluidised bed combustor focusing on gaseous emissions and temperature  
606 profiles. *Energy*, 2017. 141: p. 2069-2080.

607 6. Sarkar, M., et al., Gasification performance of switchgrass pretreated with torrefaction and  
608 densification. *Applied energy*, 2014. 127: p. 194-201.

609 7. Chen, J., et al., Analysis of biomass gasification in bubbling fluidized bed with two-fluid  
610 model. *Journal of Renewable and Sustainable Energy*, 2016. 8(6): p. 063105.

611 8. Vassilev, S.V., C.G. Vassileva, and V.S. Vassilev, Advantages and disadvantages of  
612 composition and properties of biomass in comparison with coal: An overview. *Fuel*, 2015.  
613 158: p. 330-350.

614 9. Sheth, P.N. and B. Babu, Production of hydrogen energy through biomass (waste wood)  
615 gasification. *International Journal of Hydrogen Energy*, 2010. 35(19): p. 10803-10810.

616 10. Yılmaz, S. and H. Selim, A review on the methods for biomass to energy conversion  
617 systems design. *Renewable and Sustainable Energy Reviews*, 2013. 25: p. 420-430.

618 11. IEA., *World Energy Outlook 2013*. 2013, IEA Publications Paris.

619 12. Manatura, K., et al., Exergy analysis on torrefied rice husk pellet in fluidized bed  
620 gasification. *Applied Thermal Engineering*, 2017. 111: p. 1016-1024.

621 13. Husmann, M., et al., Comparison of dolomite and lime as sorbents for in-situ H<sub>2</sub>S removal  
622 with respect to gasification parameters in biomass gasification. *Fuel*, 2016. 181: p. 131-  
623 138.

624 14. Đurišić-Mladenović, N., B.D. Škrbić, and A. Zabaniotou, Chemometric interpretation of  
625 different biomass gasification processes based on the syngas quality: Assessment of crude  
626 glycerol co-gasification with lignocellulosic biomass. *Renewable and Sustainable Energy*  
627 *Reviews*, 2016. 59: p. 649-661.

628 15. Ruiz, J., et al., Biomass gasification for electricity generation: review of current technology  
629 barriers. *Renewable and Sustainable Energy Reviews*, 2013. 18: p. 174-183.

630 16. Couto, N., et al., Influence of the biomass gasification processes on the final composition  
631 of syngas. *Energy Procedia*, 2013. 36: p. 596-606.

- 632 17. Patra, T.K. and P.N. Sheth, Biomass gasification models for downdraft gasifier: A state-  
633 of-the-art review. *Renewable and Sustainable Energy Reviews*, 2015. 50: p. 583-593.
- 634 18. Karmakar, M., et al., Investigation of fuel gas generation in a pilot scale fluidized bed  
635 autothermal gasifier using rice husk. *Fuel*, 2013. 111: p. 584-591.
- 636 19. Subbaiah, B.S., et al., Gasification of biomass using fluidized bed. *International Journal of*  
637 *Innovative Research in Science, Engineering and Technology*, 2014. 3(2): p. 8995-9002.
- 638 20. Singh, D., et al., Groundnut shell gasification performance in a fluidized bed gasifier with  
639 bubbling air as gasification medium. *Environmental technology*, 2018: p. 1-13.
- 640 21. Sarker, S., et al., Characterization and pilot scale fluidized bed gasification of herbaceous  
641 biomass: a case study on alfalfa pellets. *Energy Conversion and Management*, 2015. 91: p.  
642 451-458.
- 643 22. Maglinao Jr, A.L., S.C. Capareda, and H. Nam, Fluidized bed gasification of high tonnage  
644 sorghum, cotton gin trash and beef cattle manure: evaluation of synthesis gas production.  
645 *Energy conversion and management*, 2015. 105: p. 578-587.
- 646 23. Hosseini, S.E., et al., A review on biomass-based hydrogen production for renewable  
647 energy supply. *International Journal of Energy Research*, 2015. 39(12): p. 1597-1615.
- 648 24. Kook, J.W., et al., Gasification and tar removal characteristics of rice husk in a bubbling  
649 fluidized bed reactor. *Fuel*, 2016. 181: p. 942-950.
- 650 25. Mohammed, M., et al., Air gasification of empty fruit bunch for hydrogen-rich gas  
651 production in a fluidized-bed reactor. *Energy Conversion and Management*, 2011. 52(2):  
652 p. 1555-1561.
- 653 26. Ściążko, M. and L. Stępień, A Modified Gibbs Free Energy Minimisation Model for Fluid  
654 Bed Coal Gasification. *Chemical and Process Engineering*, 2015. 36(1): p. 73-87.
- 655 27. Pumiglia, D., et al., Aggravated test of Intermediate temperature solid oxide fuel cells fed  
656 with tar-contaminated syngas. *Journal of Power Sources*, 2017. 340: p. 150-159.
- 657 28. Woytiuk, K., et al., The effect of torrefaction on syngas quality metrics from fluidized bed  
658 gasification of SRC willow. *Renewable Energy*, 2017. 101: p. 409-416.
- 659 29. Wolff, D., E. Walsh, and K. McDonnell, Practical experience with woody biomass in a  
660 down-draft gasifier. *Journal of Technology Innovations in Renewable Energy*, 2013. 2(1):  
661 p. 47-52.
- 662 30. Volk, T.A., J.P. Heavey, and M.H. Eisenbies, Advances in shrub-willow crops for  
663 bioenergy, renewable products, and environmental benefits. *Food and Energy Security*,  
664 2016. 5(2): p. 97-106.
- 665 31. Serapiglia, M.J., et al., Yield and woody biomass traits of novel shrub willow hybrids at  
666 two contrasting sites. *BioEnergy Research*, 2013. 6(2): p. 533-546.
- 667 32. García, R., et al., Biomass proximate analysis using thermogravimetry. *Bioresource*  
668 *technology*, 2013. 139: p. 1-4.
- 669 33. Nyakuma, B.B., et al., Thermogravimetric analysis of the fuel properties of empty fruit  
670 bunch briquettes. *Jurnal Teknologi*, 2014. 67(3).

- 671 34. Pottmaier, D., et al., The profiles of mass and heat transfer during pinewood conversion.  
672 Energy Procedia, 2015. 66: p. 285-288.
- 673 35. González-Vázquez, M.P., et al., Comparison of the gasification performance of multiple  
674 biomass types in a bubbling fluidized bed. Energy Conversion and Management, 2018.  
675 176: p. 309-323.
- 676 36. Motta, I.L., et al., Biomass gasification in fluidized beds: A review of biomass moisture  
677 content and operating pressure effects. Renewable and Sustainable Energy Reviews, 2018.  
678 94: p. 998-1023.
- 679 37. Li, G., et al., Modeling of ash agglomerating fluidized bed gasifier using back propagation  
680 neural network based on particle swarm optimization. Applied Thermal Engineering, 2018.  
681 129: p. 1518-1526.
- 682 38. Jordan, C.A. and G. Akay, Speciation and distribution of alkali, alkali earth metals and  
683 major ash forming elements during gasification of fuel cane bagasse. Fuel, 2012. 91(1): p.  
684 253-263.
- 685 39. Ma, Z., et al., Gasification of rice husk in a downdraft gasifier: the effect of equivalence  
686 ratio on the gasification performance, properties, and utilization analysis of byproducts of  
687 char and tar. BioResources, 2015. 10(2): p. 2888-2902.
- 688 40. Adnan, M.A., et al., Gasification performance of Spirulina microalgae—A thermodynamic  
689 study with tar formation. Fuel, 2019. 241: p. 372-381.
- 690 41. Basu, P., Biomass gasification and pyrolysis: practical design and theory. 2010: Academic  
691 press.
- 692 42. Varma, A.K. and P. Mondal, Physicochemical characterization and pyrolysis kinetic study  
693 of sugarcane bagasse using thermogravimetric analysis. Journal of Energy Resources  
694 Technology, 2016. 138(5): p. 052205.
- 695 43. Nyakuma, B.B., et al. Thermogravimetric Analysis of Char Waste from the Air  
696 Gasification of Empty Fruit Bunch Briquette. in MATEC Web of Conferences. 2014. EDP  
697 Sciences.
- 698 44. Nyakuma, B.B., et al., Comparative analysis of the calorific fuel properties of Empty Fruit  
699 Bunch Fiber and Briquette. Energy Procedia, 2014. 52: p. 466-473.
- 700 45. Ahmad, A.A., et al., Assessing the gasification performance of biomass: A review on  
701 biomass gasification process conditions, optimization and economic evaluation.  
702 Renewable and Sustainable Energy Reviews, 2016. 53: p. 1333-1347.
- 703 46. Zhao, J., et al., TG–DSC analysis of straw biomass pyrolysis and release characteristics of  
704 noncondensable gas in a fixed-bed reactor. Drying technology, 2017. 35(3): p. 347-355.
- 705 47. Kaewluan, S. and S. Pipatmanomai, Potential of synthesis gas production from rubber  
706 wood chip gasification in a bubbling fluidised bed gasifier. Energy conversion and  
707 management, 2011. 52(1): p. 75-84.
- 708 48. Kim, Y.D., et al., Air-blown gasification of woody biomass in a bubbling fluidized bed  
709 gasifier. Applied energy, 2013. 112: p. 414-420.

- 710 49. Guo, F., et al., Effect of design and operating parameters on the gasification process of  
711 biomass in a downdraft fixed bed: An experimental study. *International Journal of*  
712 *Hydrogen Energy*, 2014. 39(11): p. 5625-5633.
- 713 50. Monteiro, E., et al., Experimental and modeling studies of Portuguese peach stone  
714 gasification on an autothermal bubbling fluidized bed pilot plant. *Energy*, 2018. 142: p.  
715 862-877.
- 716 51. González-Vázquez, M.d.P., et al., Unconventional biomass fuels for steam gasification:  
717 Kinetic analysis and effect of ash composition on reactivity. *Energy*, 2018. 155: p. 426-  
718 437.
- 719 52. Karatas, H. and F. Akgun, Experimental results of gasification of walnut shell and pistachio  
720 shell in a bubbling fluidized bed gasifier under air and steam atmospheres. *Fuel*, 2018. 214:  
721 p. 285-292.
- 722 53. Pérez, N.P., et al., Fluid-dynamic assessment of sugarcane bagasse to use as feedstock in  
723 bubbling fluidized bed gasifiers. *Applied thermal engineering*, 2014. 73(1): p. 238-244.
- 724 54. Gao, N., A. Li, and C. Quan, A novel reforming method for hydrogen production from  
725 biomass steam gasification. *Bioresource technology*, 2009. 100(18): p. 4271-4277.
- 726 55. Acharya, B., A. Dutta, and P. Basu, An investigation into steam gasification of biomass for  
727 hydrogen enriched gas production in presence of CaO. *International Journal of Hydrogen*  
728 *Energy*, 2010. 35(4): p. 1582-1589.
- 729 56. Liu, L., et al., Experimental study of biomass gasification with oxygen-enriched air in  
730 fluidized bed gasifier. *Science of the Total Environment*, 2018. 626: p. 423-433.
- 731 57. Diyoke, C., et al., Modelling of down-draft gasification of biomass—An integrated  
732 pyrolysis, combustion and reduction process. *Applied Thermal Engineering*, 2018. 142: p.  
733 444-456.
- 734 58. Rapagnà, S., et al., Steam-gasification of biomass in a fluidised-bed of olivine particles.  
735 *Biomass and Bioenergy*, 2000. 19(3): p. 187-197.
- 736 59. Makwana, J., et al., Air gasification of rice husk in bubbling fluidized bed reactor with bed  
737 heating by conventional charcoal. *Bioresource technology*, 2015. 178: p. 45-52.
- 738 60. Kaewluan, S. and S. Pipatmanomai, Gasification of high moisture rubber woodchip with  
739 rubber waste in a bubbling fluidized bed. *Fuel Processing Technology*, 2011. 92(3): p. 671-  
740 677.
- 741 61. Meng, F., et al., Effect of gasifying agents on sawdust gasification in a novel pilot scale  
742 bubbling fluidized bed system. *Fuel*, 2019. 249: p. 112-118.
- 743 62. Shehzad, A., et al., Modeling and comparative assessment of bubbling fluidized bed  
744 gasification system for syngas production—a gateway for a cleaner future in Pakistan.  
745 *Environmental technology*, 2018. 39(14): p. 1841-1850.
- 746 63. Hamad, M.A., et al., Hydrogen rich gas production from catalytic gasification of biomass.  
747 *Renewable Energy*, 2016. 85: p. 1290-1300.
- 748 64. Ahmed, R., et al., Thermodynamics analysis of refinery sludge gasification in adiabatic  
749 updraft gasifier. *The Scientific World Journal*, 2014. 2014.

750

751

## List of Tables

752

753

754

755

756

**Table 1.** Proximate and ultimate analysis of SRC willow chips.

Biomass fuel	Ultimate analysis (wt %) <sup>a</sup>					Proximate analysis (wt %) <sup>c</sup>				
	C	H	N	O <sup>b</sup>	S	M	VM	FC	Ash	LHV(MJ/m <sup>3</sup> )
SRC willow chips	45.4	5.7	0.8	48	0.1	2.9	82.5	12.9	1.7	4.4

757

758 M - Moisture; VM - Volatile matter; FC - Fixed carbon.

759 <sup>a</sup> On dry-ash-free basis.

760 <sup>b</sup> Calculated by the difference.

761 <sup>c</sup> On dry basis except for moisture which is on an as received basis.

762 <sup>d</sup> Low heating value (dry)

763

764  
765  
766  
767  
768  
769

**Table 2.** Operating conditions of bubbling fluidized bed biomass gasifier (BFBBG).

Equivalent Ratio (ER)	0.25, 0.29 and 0.32
Gasification air flow rate (L/m)	45, 65, 80
Hopper air flow rate (L/m)	3
Fluidization velocity (m/s)	<5
Feeding rate (g/h)	2469.6, 2126.8 and 1920.9
Heater temperature setup (°C)	650–850
Screw feeder motor frequency (Hz)	10, 11, 12.5
Silica sand particle size	
Dimension (µm)	212–300
Density (kg/m <sup>3</sup> )	1520

770  
771



772

773

774

775

776

777

**Table 3.** Major reactions of gasification.

Reaction name	Reactions	$\Delta H^0$ (KJ/mol)
Oxidation	$C(s)+O_2 \leftrightarrow CO_2$	-394.0 <sup>a</sup>
	$C(s)+1/2O_2 \leftrightarrow CO$	-123.0 <sup>a</sup>
Boudouard	$C(s)+CO_2 \leftrightarrow 2CO$	+172.0 <sup>b</sup>
Water gas	$C(s)+H_2O \leftrightarrow CO+H_2$	+131.0 <sup>b</sup>
	$C(s)+2H_2O \leftrightarrow CO_2+2H_2$	+771.0 <sup>b</sup>
Methanation	$C(s)+2H_2 \leftrightarrow CH_4$	-87.0 <sup>a</sup>
Water gas shift	$CO+H_2O \leftrightarrow CO_2+H_2$	-41.0 <sup>a</sup>
Steam reforming	$CH_4+H_2O \leftrightarrow CO+3H_2$	+206.0 <sup>b</sup>

778

779 <sup>a</sup> Negative sign indicates the exothermic reactions.780 <sup>b</sup> Positive sign indicates the endothermic reactions.

781

782

783

784

**Table 4.** Product gas analysis and gasifier performance of SRC willow chips

<b>Feedstock</b>	<b>SRC willow chips</b>		
<b>ER</b>	0.25	0.29	0.32
<b>Feeding rate (g/h)</b>	2469.6	2126.8	1920.9
<b>Product gas composition (Vol %)</b>			
H <sub>2</sub>	9.95 <sup>a</sup>	8.26 <sup>a</sup>	6.30 <sup>a</sup>
	8.96 <sup>b</sup>	8.31 <sup>b</sup>	6.53 <sup>b</sup>
CO	16.98 <sup>a</sup>	14.20 <sup>a</sup>	12.72 <sup>a</sup>
	16.64 <sup>b</sup>	14.50 <sup>b</sup>	12.29 <sup>b</sup>
CH <sub>4</sub>	4.43 <sup>a</sup>	3.94 <sup>a</sup>	3.88 <sup>a</sup>
	4.67 <sup>b</sup>	4.06 <sup>b</sup>	4.22 <sup>b</sup>
CO <sub>2</sub>	17.49 <sup>a</sup>	18.16 <sup>a</sup>	19.21 <sup>a</sup>
	17.99 <sup>b</sup>	18.16 <sup>b</sup>	18.24 <sup>b</sup>
LHV (MJ/m <sup>3</sup> )	4.37	3.89	3.67
CGE (%)	49.63	47.89	46.43
CCE (%)	90.68	95.48	95.76
Gas yield (m <sup>3</sup> /h)	3.93	4.17	4.55
Tar yield (g/m <sup>3</sup> )	16.78	12.45	7.24

785 Online analysis<sup>a</sup>786 GC analysis<sup>b</sup>

# List of Figures

787  
788  
789  
790  
791  
792

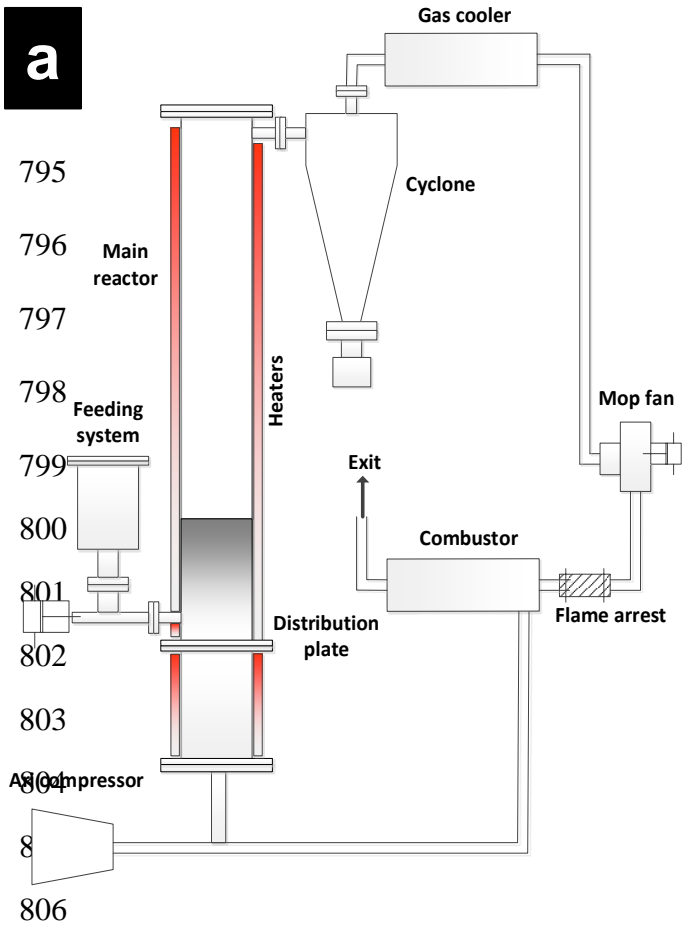


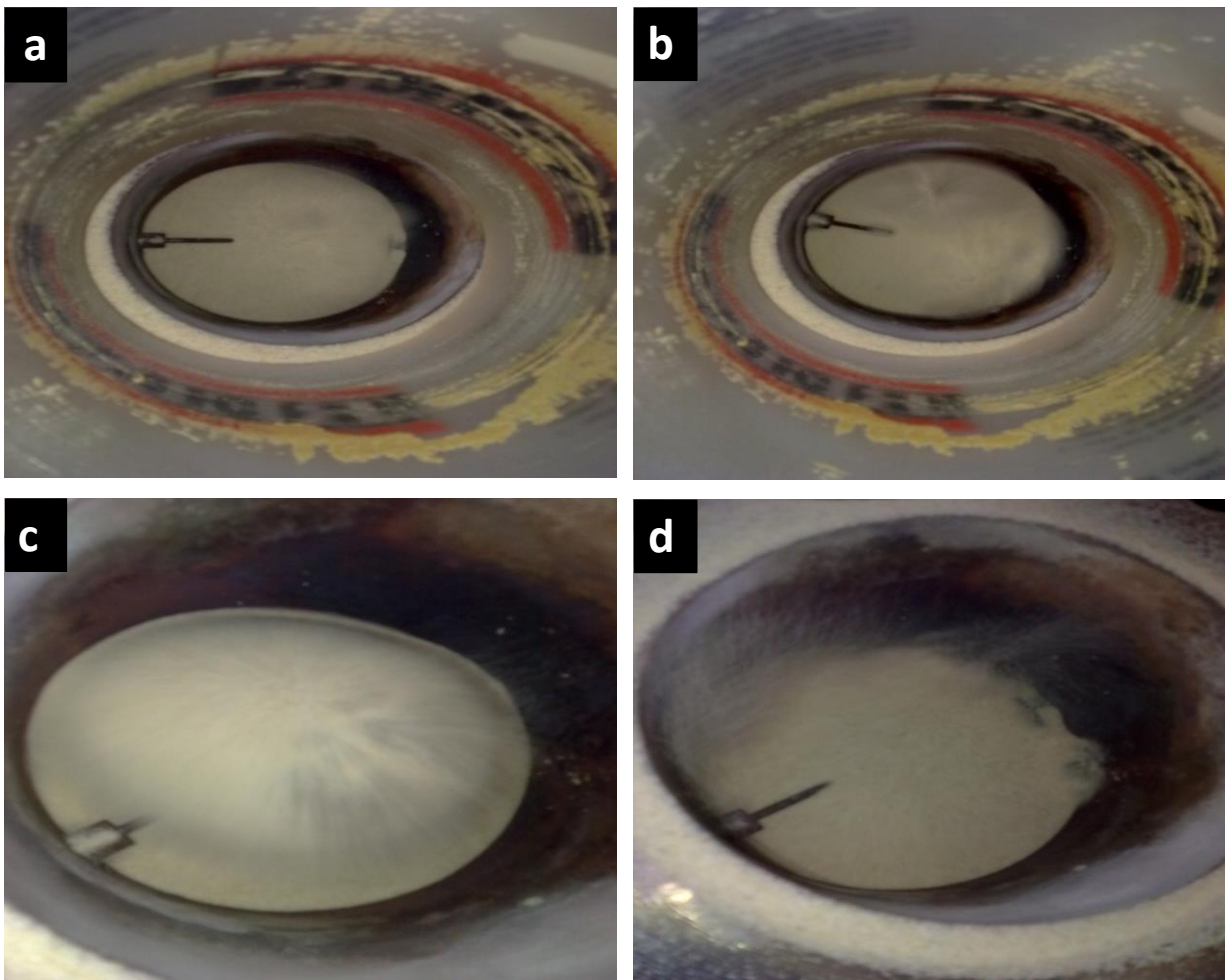
**Fig. 1.** (a) Schematic diagram of bubbling fluidized bed biomass gasifier; (b) Experimental set up of bubbling fluidized bed reactor and cyclone.

810

811

812

813

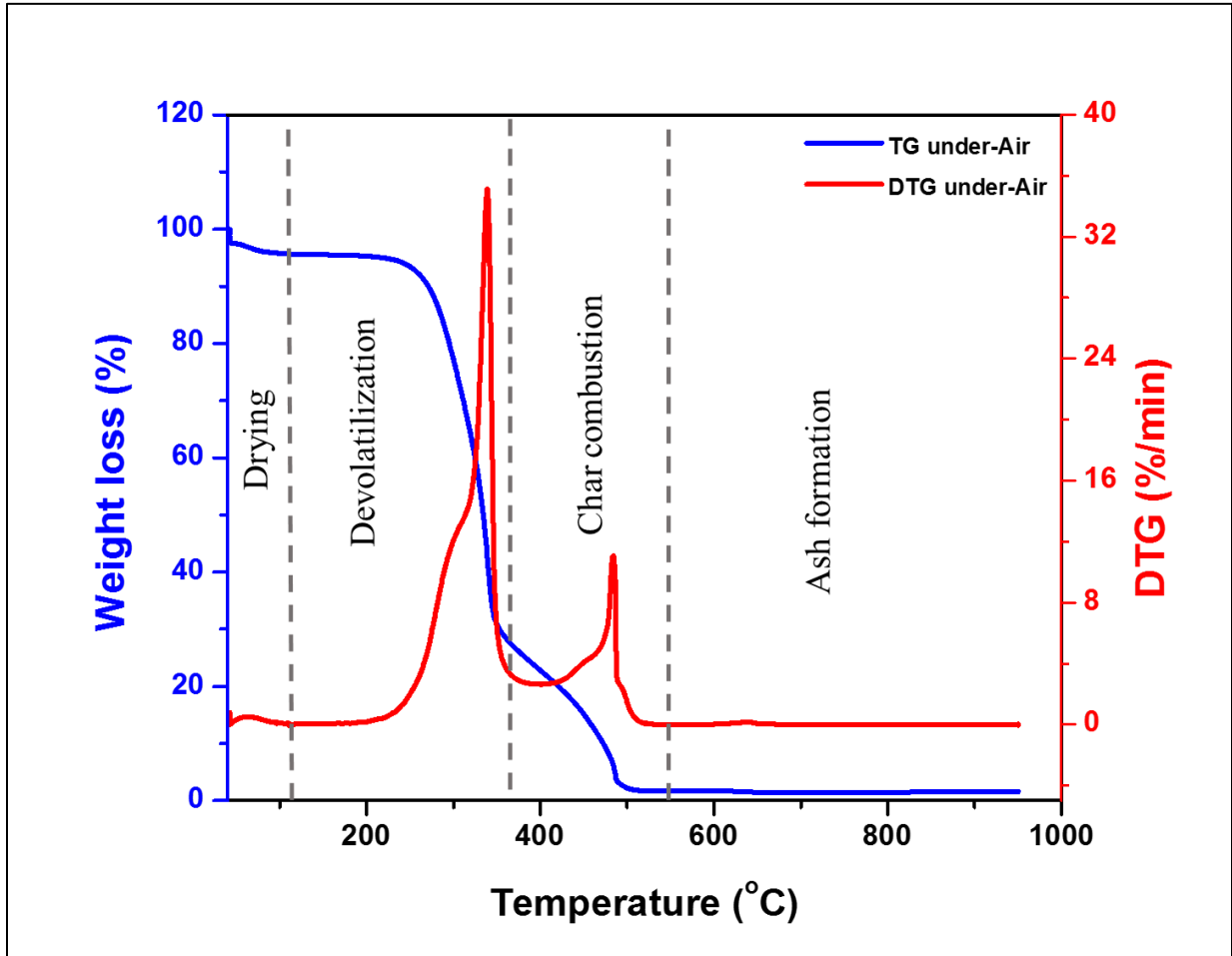


814

815 **Fig. 2.** (a) Bed material in the reactor, (b) Bubble initiation in the reactor, (c) Air bubble rising in  
816 the reactor and (d) Air bubble burst in the reactor.

817

818  
819  
820  
821  
822



823  
824  
825

Fig. 3. TG/DTG curves of SRC willow woodchips under air.

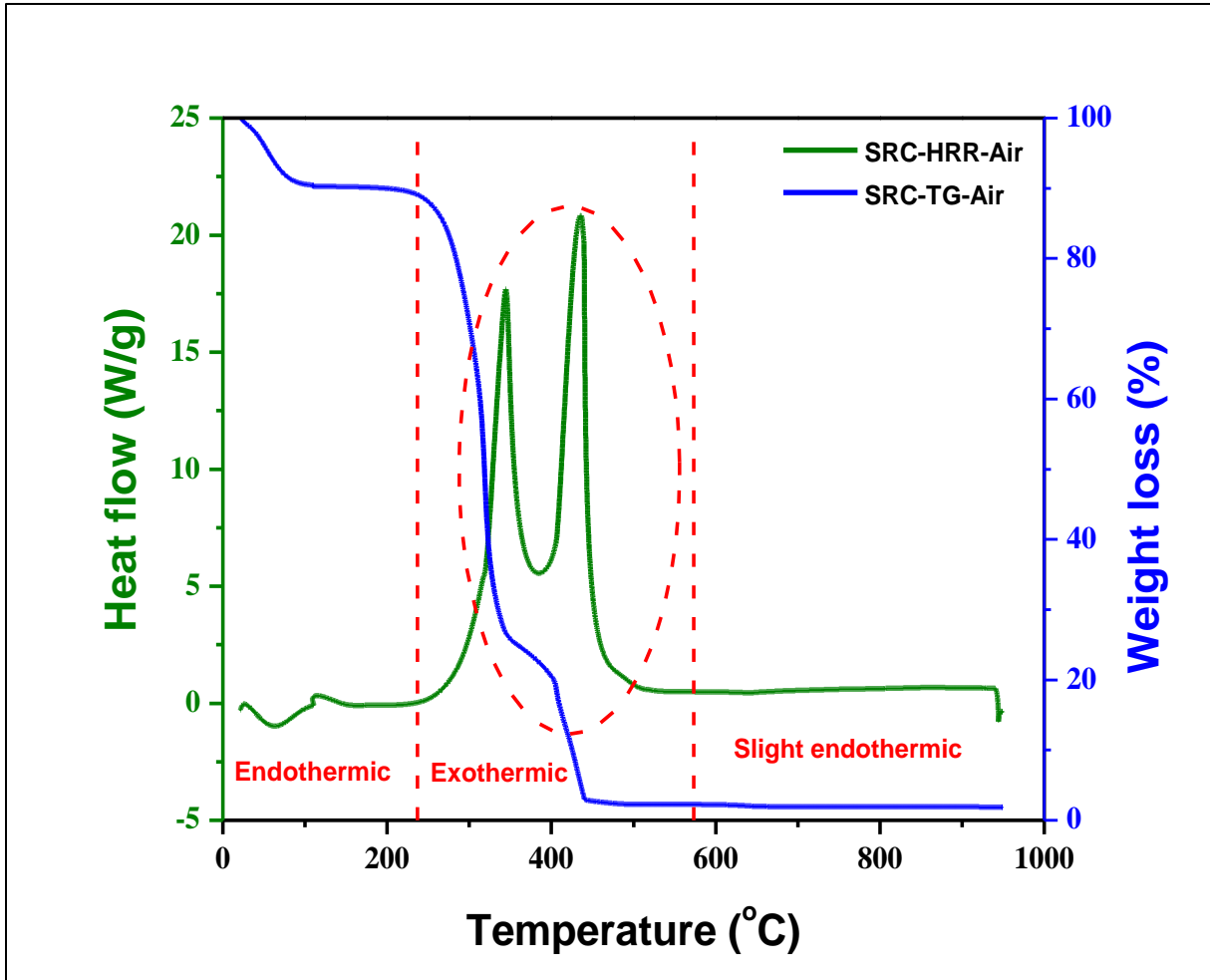
826

827

828

829

830



831

832

833

**Fig. 4.** Heat transfer profile of SRC willow woodchips conversion under air.

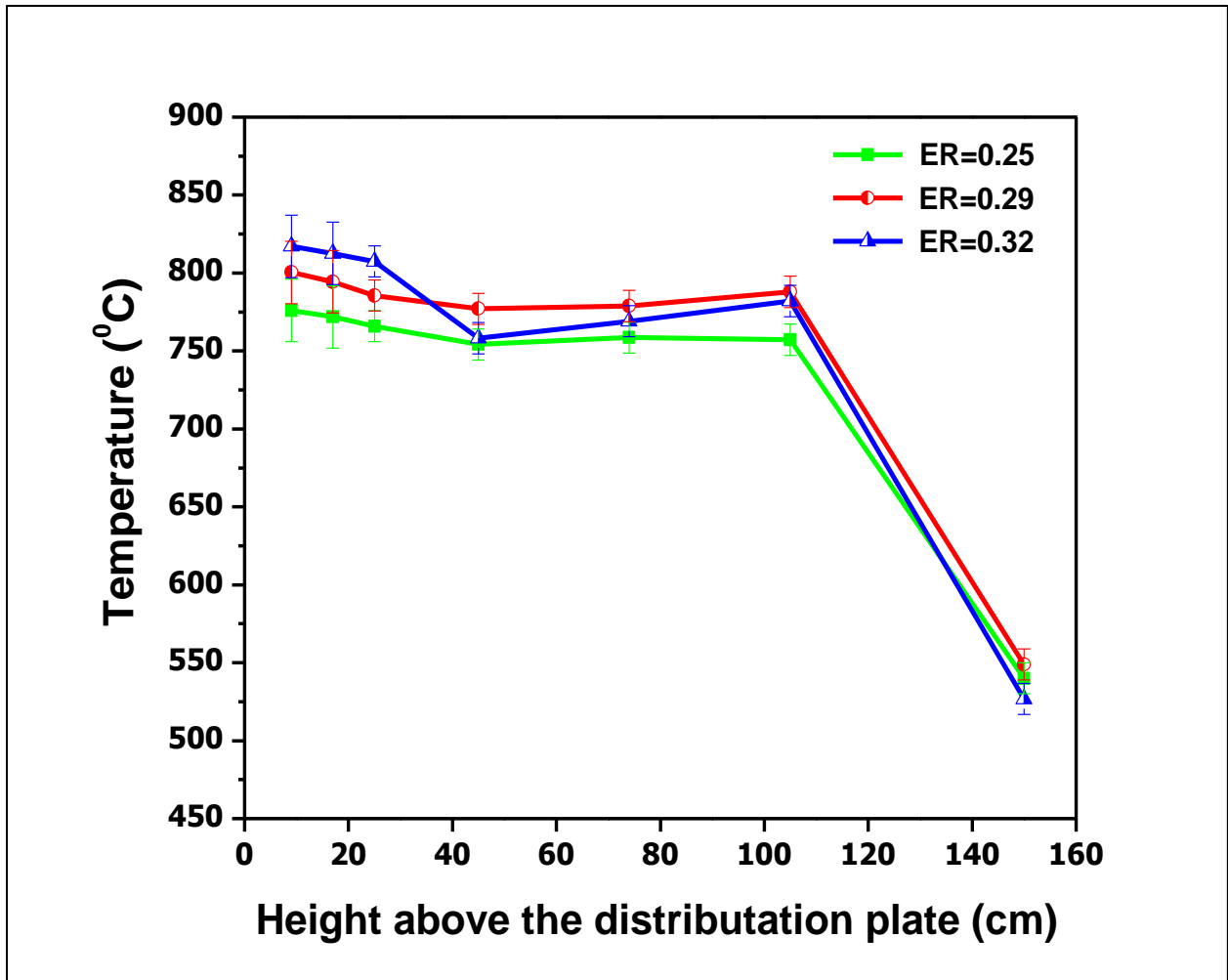
834

835

836

837

838



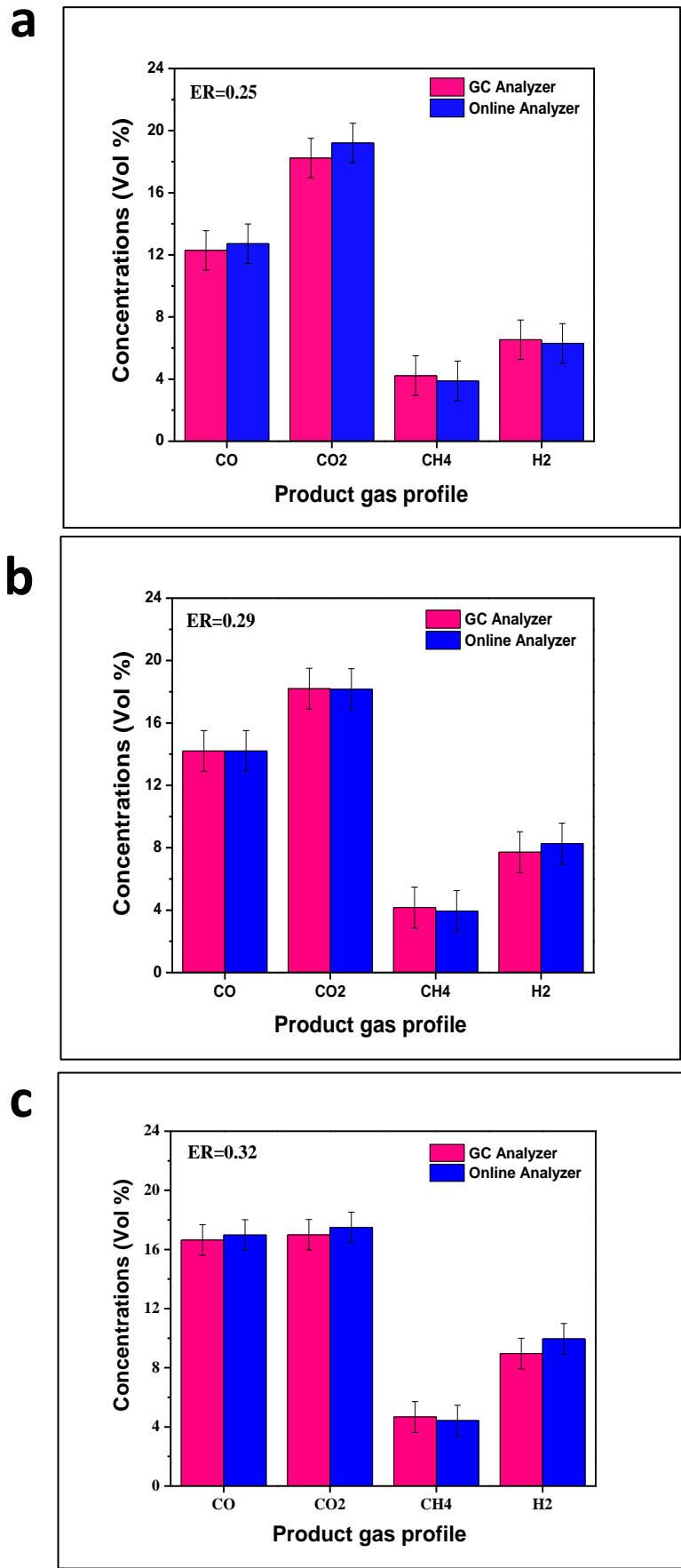
839

840

841

Fig. 5. Effect of temperature along the height of reactor at different ERs.

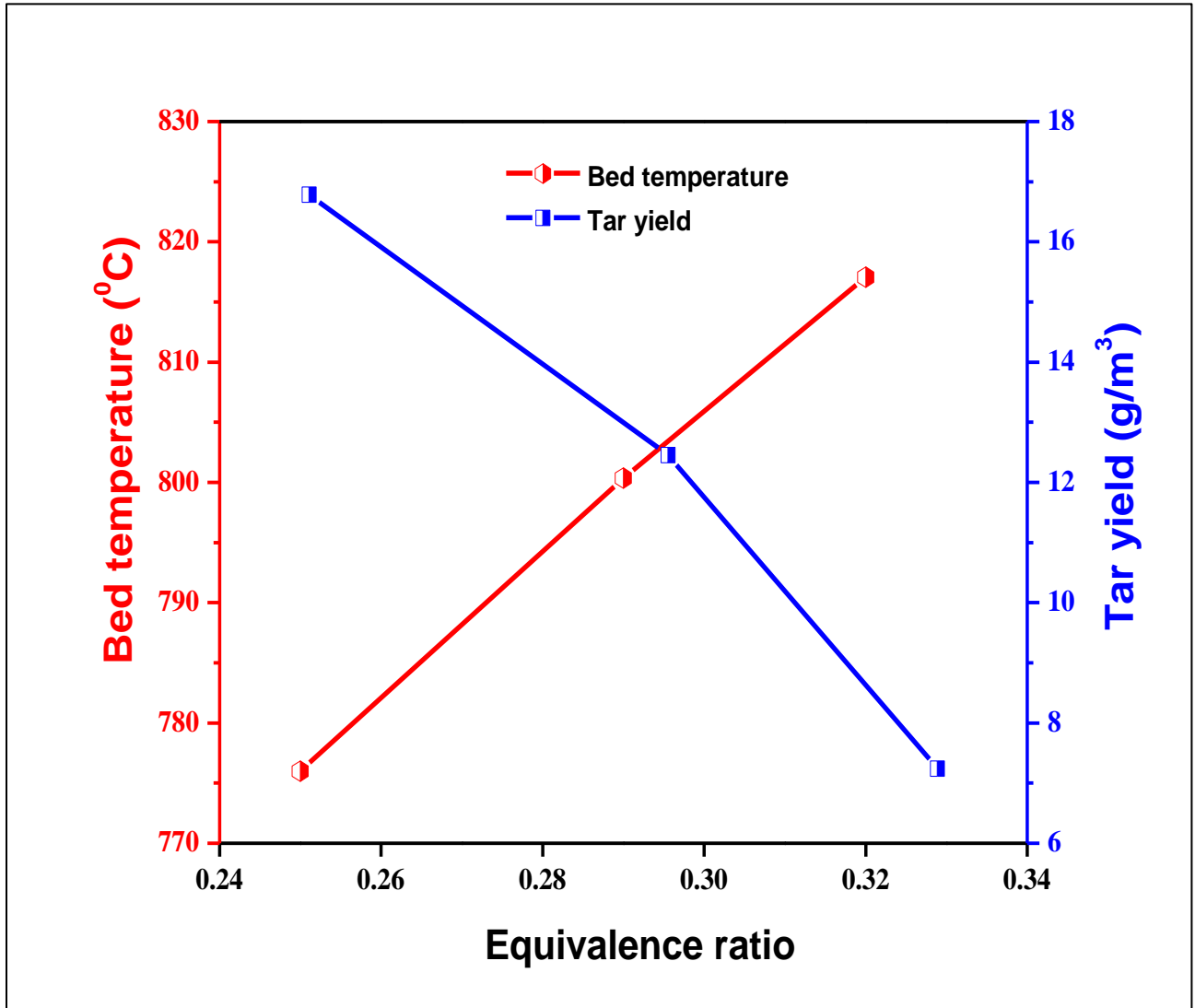
842  
843  
844  
845  
846  
847  
848  
849  
850  
851  
852  
853  
854  
855  
856  
857  
858  
859  
860  
861  
862  
863  
864  
865  
866



867 **Fig. 6.** Effect of different equivalence ratios on the product gas concentrations along with the  
868 comparison of GC and online analysis; (a) 0.25 ER, (b) 0.29 ER and (c) 0.32 ER.



869  
870  
871  
872



873  
874  
875

**Fig. 7.** Effect of equivalence ratio (ER) on bed temperature and tar yield.

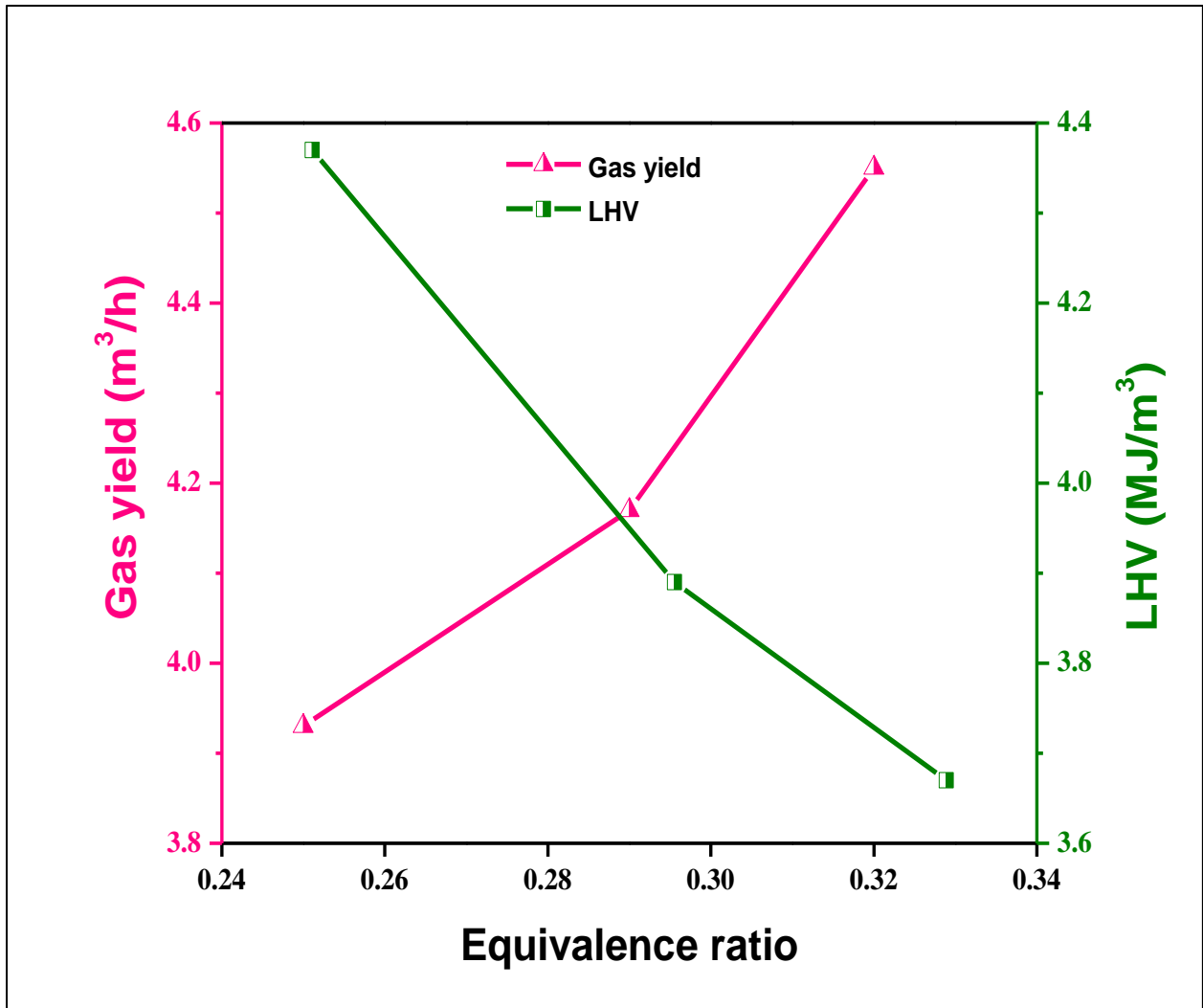
876

877

878

879

880



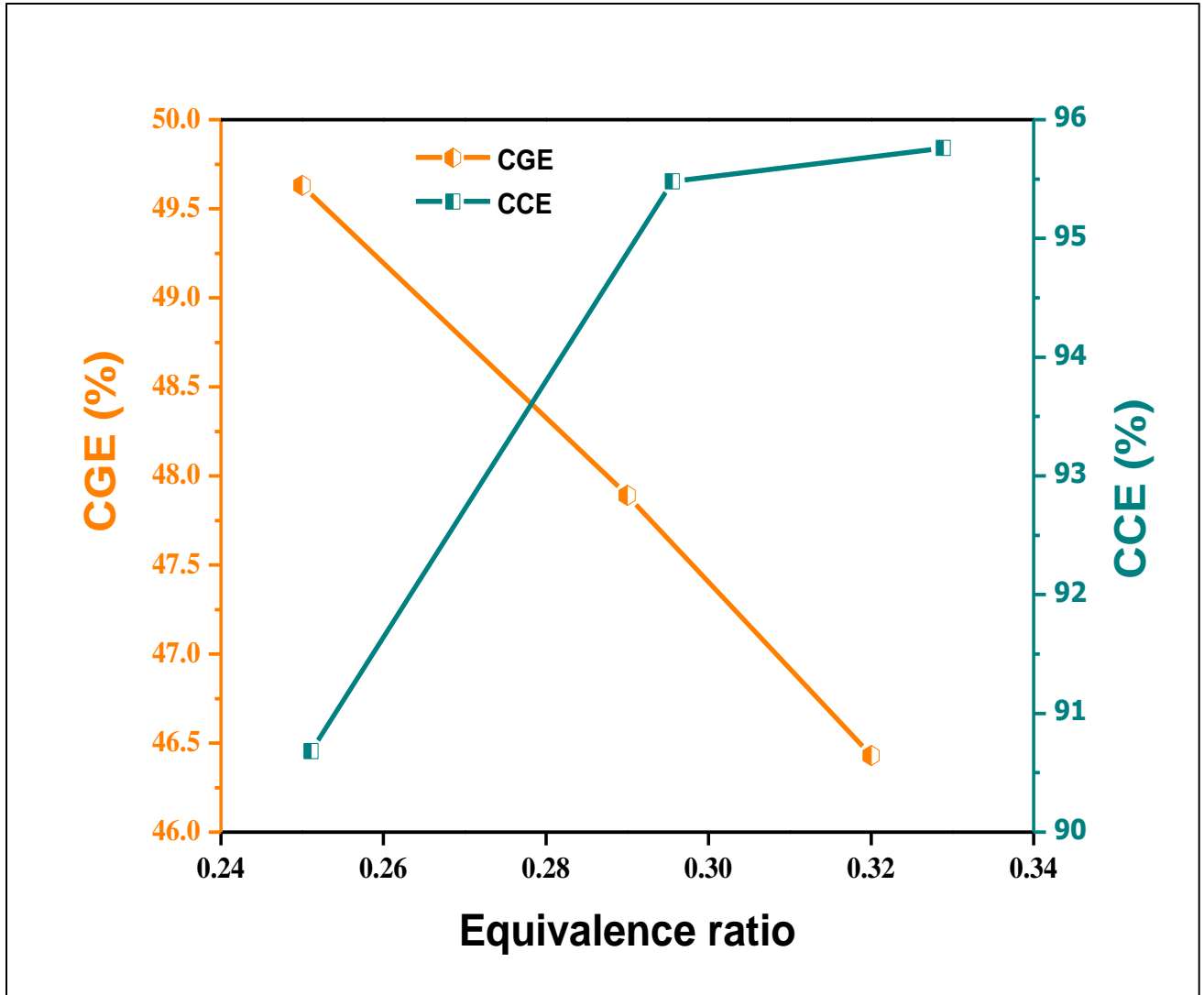
881

882

883

**Fig. 8.** Effect of equivalence ratio (ER) on gas yield and LHV.

884  
885  
886  
887  
888



889  
890  
891  
892

**Fig. 9.** Effect of equivalence ratio (ER) on CGE and CCE.